BBA - General Subjects 1863 (2019) 1–12

Contents lists available at ScienceDirect

BBA - General Subjects

journal homepage: www.elsevier.com/locate/bbagen

Myrtenal-induced V-ATPase inhibition - A toxicity mechanism behind tumor cell death and suppressed migration and invasion in melanoma

Brunna Xavier Martins[a], Raul Ferraz Arruda[a], Gildeíde Aparecida Costa[a], Hassan Jerdy[b], Sávio Bastos de Souza[a], Julianna Maria Santos[a,1], William Rodrigues de Freitas[c], Milton Masahiko Kanashiro[c], Eulógio Carlos Queiroz de Carvalho[b], Nadir Francisca Sant'Anna[a], Fernanda Antunes[b,d], Raul Martinez-Zaguilan[e], Sennoune Souad[e], Anna Lvovna Okorokova-Façanha[d,f], Arnoldo Rocha Façanha[a,d,*]

[a] *Laboratório de Biologia Celular e Tecidual, Centro de Biociências e Biotecnologia, Universidade Estadual do Norte Fluminense Darcy Ribeiro, Campos dos Goytacazes, Rio de Janeiro, Brazil*

[b] *Hospital Veterinário/Laboratório de Morfologia e Patologia Animal, Centro de Ciências e Tecnologias Agropecuárias, Universidade Estadual do Norte Fluminense Darcy Ribeiro, Campos dos Goytacazes, Rio de Janeiro, Brazil*

[c] *Laboratório de Biologia de Reconhecer, Centro de Biociências e Biotecnologia, Universidade Estadual do Norte Fluminense Darcy Ribeiro, Campos dos Goytacazes, Rio de Janeiro, Brazil*

[d] *Unidade de Experimentação Animal (UEA), Universidade Estadual do Norte Fluminense Darcy Ribeiro, Campos dos Goytacazes, Rio de Janeiro, Brazil*

[e] *Texas Tech University, Department of Physiology, Health Sciences Center, Lubbock, TX, USA*

[f] *Laboratório de Bioquímica e Fisiologia de Microrganismos, Centro de Biociências e Biotecnologia, Universidade Estadual do Norte Fluminense Darcy Ribeiro, Campos dos Goytacazes, Rio de Janeiro, Brazil*

ARTICLE INFO

Keywords:
Proton pumps inhibitors
Anti-melanoma drugs
Bioactive terpenes
pH signatures
Tumor acidification

ABSTRACT

Background: Metastatic tumor cells have acidic extracellular pH and differential electrochemical H^+ gradients generated across their cell membranes by V-type H^+-ATPases. This study shows that inhibition of the V-ATPases by the plant-derived monoterpene Myrtenal results in tumor cell death and decreased metastatic dissemination in mice.

Methods: The Myrtenal anticancer toxicity was evaluated *in vitro* using murine (B16F0 and B16F10) and human (SkMel-5) melanoma cell lines, and in *in vivo* mouse metastatic dissemination model. Proton flux and extracellular acidification were directly evaluated at the surface of living cells using a non-invasive selective ion electrode approach.

Results: The inhibition of V-ATPases by 100 μM Myrtenal disrupted the electrochemical H^+ gradient across the cell membranes, strongly induced cell death (4–5 fold), and decreased tumor cells migration and invasion *in vitro*. Myrtenal (15 mg/kg) also significantly reduced metastasis induced by B16F10 *in vivo*, further reinforcing that V-ATPase is a molecular target to halt the progression of cancers.

Conclusions: These data revealed the therapeutic potential of Myrtenal as inhibitor of melanoma progression proposing a mechanism of action by which once inhibited by this monoterpene the proton pumps fail to activate cancer-related differential electrochemical gradients and H^+ fluxes across the tumor cell membranes, disrupting pH signatures inherent in tumor progression, resulting in reprogrammed cell death and metastasis inhibition.

General significance: The work represents a new mechanistic strategy for contention of melanoma, the most aggressive and deadly form of cutaneous neoplasm, and highlights Myrtenal, other related monoterpenes and derivatives as promising proton pump inhibitors with high chemotherapeutic potential.

* Corresponding author: Laboratório de Biologia Celular e Tecidual, Centro de Biociências e Biotecnologia, Universidade Estadual do Norte Fluminense Darcy Ribeiro. Campos dos Goytacazes-RJ, Brazil.
E-mail address: arnoldo@uenf.br (A.R. Façanha).
[1] Current address: Texas Tech University, Mechanical Engineering Department, Lubbock, TX, USA.

https://doi.org/10.1016/j.bbagen.2018.09.006
Received 11 February 2018; Received in revised form 9 September 2018; Accepted 10 September 2018
Available online 11 September 2018

1. Introduction

Over the years, many synthetic and natural plant compounds have been considered as potential anti-neoplastic drugs and have increasingly been used alone or in combination with conventional chemotherapeutic agents [1,2]. Myrtenal is an active principle of essential oils found in plants, such as cardamom, orange, lemon, spearmint, pepper and ginger, widely used as flavoring agent in food industry [3], for which no toxicity mechanism has been demonstrated up to now. Here, we provide a body of evidence that demonstrate a new bioactivity for this monoterpene, associated with a strong antimelanoma activity mechanistically related to the inhibition of V-ATPases, a molecular target that have been increasingly demonstrated to be overexpressed in tumor membranes of highly metastatic cancer cells [4,5].

Significant advances have been achieved in cancer therapy, leading to an improvement of overall patient survival and reduction of mortality rates in some, but not all types of cancer. Malignant melanoma, the most lethal skin cancer, evades most pro-apoptotic mechanisms and has shown an increase in death incidence over the last decades [6]. Progress in the treatment of this lethal disease has been made by using immunotherapy with Ipilimumab, a human monoclonal antibody that targets cytotoxic T-lymphocyte antigen 4 (CTLA-4), which was found to be effective in only 11% of the cases. Another chemotherapy drug, Vemurafenib, has shown to improve overall survival in 40–50%, but just for those patients with specific V600E mutation in the BRAF enzyme [7,8]. Therefore, new bioactive molecules with wider therapeutic spectrum are required for development of more effective and safer antimelanoma therapies.

In 1956, Otto Warburg reported that tumors generated an acidic extracellular microenvironment as result of increased glycolysis and other related changes in cancer bioenergetics [9]. However, only recently has this feature become a major focus to develop novel approaches for cancer therapy [10]. A series of seminal studies has uncovered that extracellular tumor acidification increases the malignant phenotype of tumor cells, by activating proteases with optima acidic extracellular pH that disrupts the extracellular matrix and contributes to tumor cell invasion and dissemination of highly metastatic tumors [11–13]. These works have proved that tumor acidification is associated with differential activations of V-type H^+-ATPases (V-ATPases), transmembrane ATP-dependent proton pumps composed by a multisubunit complex that energizes a myriad of secondary transport systems across cell membranes, pumping H^+ ions from the cytoplasm into the lumen of organelles or to the extracellular matrix [14]. Chronic disturbances of cellular and extracellular ionic homeostasis, and alterations in energy metabolism in carcinogenic processes are main factors in tumor progression, invasion and metastasis [15]. Alterations in pH are also involved in DNA damage and control of programmed cell death [16,17]. Tumor cells express differential electrochemical gradient of ions in their cell membranes, including the nuclear membranes, driven by V-ATPases [18], which has been linked to the apoptosis avoidance [16] and metastasis [15]. Recently, we have also demonstrated that disturbance of membrane microdomains promotes V-ATPase inhibition and disrupts pH signatures required for melanoma cell migration and invasion [19].

In this work, a putative anti-metastatic potential of the monoterpene Myrtenal is investigated through a toxicity/therapeutic mechanism of action by which inhibition of V-ATPase will induce programmed cell death and inhibit migration and invasiveness *in vitro* in human and mice tumor cell lines, inhibiting metastatic dissemination *in vivo* in a mouse melanoma model.

2. Materials and methods

2.1. Chemicals

(1*R*)-(-)-Myrtenal and concanamycin A purchased from Sigma Aldrich® were prepared as a stock solution in dimethyl sulfoxide (DMSO).

2.2. Cell lines and cell culture

B16F0 and B16F10 murine melanoma cell lines were used as models of low and high proliferative and metastatic potential, respectively, and compared with the highly metastatic human melanoma cell line SkMel-5. We also used a murine macrophage cell line (J774 A_1) that is known to express V-ATPase at the plasma membrane as non-cancer control cells [20] (Supplemental Fig. S2). Melanoma cell lines B16F0, B16F10 and SkMel-5 were cultured in DMEM medium (Sigma Aldrich®) supplemented with 10% FBS (Gibco™). The cells were incubated at 37 °C in a humidified chamber containing 5% CO_2. As expected, the highest metastatic cells, B16F10 and SkMel-5, exhibited a faster cell growth rate than the less metastatic B16F0 or the non-tumor J774 A_1 cell line (Supplemental Fig. S1A). The cell lines were obtained from the cell bank of the Federal University of Rio de Janeiro (UFRJ, Brazil).

2.3. Cell viability assay

The viability of the cells incubated with Myrtenal was evaluated by an MTT (3-(4,5 dimethyltiazol-2-yl)-2,5-diphenyl tetrazolium bromide) assay, as described earlier [21]. Cells were plated in 96-well plates at 8.3×10^4 cells/mL, and then were treated with different concentrations of Myrtenal (10, 20, 50, 100, and 200 μM) or concanamycin A. The formazan crystals were dissolved in acidic isopropanol and their absorbance was determined at 570 nm using a microplate reader (Thermo Labsystems Multiskan, model 352). Treatment of these cells with increasing Myrtenal concentrations (10–200 μM) for 24 h resulted in a concentration-dependent decrease in cell viability, and above 50 μM this effect was stronger in the higher metastatic melanoma cell lines B16F10 and SkMel-5 (Supplemental Fig. S1B).

2.4. Evaluation of cell death

Apoptotic and necrotic cells were quantified by double staining with acridine orange and ethidium bromide essentially as previously described [22], a method in which viable/early apoptotic cells stain green with bright green dots in the nuclei, while late apoptotic and necrotic cells exhibit increasing orange fluorescence depending on the loss of membrane integrity due to co-staining with ethidium bromide. Cells were plated in 12-well plate at a density of 1×10^5 cells/mL, and 18–20 h after adhesion the cells were treated with Myrtenal (50 μM) or concanamycin A (5 nM) and incubated at 37 °C and 5% CO_2 for 12 h. Cells were stained with 10 μg/mL acridine orange and 10 μg/mL ethidium bromide (AO/EB) and immediately examined using fluorescence microscopy (Axioplan-Carl Zeiss). In order to prevent a possible photoactivated cytotoxicity [23], straight after AO/EB incubation in the dark, the cells were quickly washed with PBS and all procedure upon white light takes no > 5–7 min and just few seconds of blue light (450–490 nm bandpass filter) exposure, no longer than is necessary to achieve the images. The resulting images were subsequently analyzed by the Zen 2.3 (Blue Edition) software.

2.5. Flow cytometry

Cells were incubated with Myrtenal (100 μM) or concanamycin A (5 nM) for 24 h. Following double staining with FITC-Annexin V and propidium iodide (PI), cells were analyzed by flow cytometry (BD FACSCalibur™) using FlowJo V10 software. The flow cytometry allowed a more detailed quantitative analysis, which distinguished early and late apoptotic cells from the necrotic cells.

2.6. Transmission electron microscopy

Cells were grown to 90% confluency and treated with 100 μM Myrtenal or 5 nM concanamycin A for 18 h and then, prepared as described by Marino et al. [24], post fixed with 1% OsO_4 in 0.12 M phosphate buffer. Cells were dehydrated in acetone and embedded in epon resin. Ultrathin sections were cut, stained with uranyl acetate and lead citrate, and analyzed in a transmission electron microscope TEM-900 (Zeiss, Germany).

2.7. Wound-healing cell migration assay

Tumor cells were plated at density of 5×10^4 cells/mL in 6-well plates and grown to 90% confluency. A wound was inflicted to the cell monolayer using a 10 μL pipette tip. The cell plates were washed with PBS for three times to remove detached cells and immediately incubated with Myrtenal (5 and 10 μM) or concanamycin A (5 nM). Images were taken at 0 and 24 h after scratching, and the wound closure was quantified.

2.8. Invasion and migration assay

For invasion assay we used the transwell system (24 wells with 8 μm pore size in polycarbonate membrane, Corning Costar). The filters were coated with 3 μg/mL Matrigel (BD Biosciences) and incubated for 3 h. Thereafter, 5×10^4 cells/mL DMEM containing 0.1% BSA and 6 μL fibronectin (10 μg/mL) were plated onto the upper chamber and grown for 24 h. Thereafter, Myrtenal (5 and 10 μM) or concanamycin A (5 nM) were added in medium into the lower chamber. After overnight incubation the cells that did not invade through the pores of the transwell inserts were removed with a cotton wool. The cells were washed with PBS and cells remained on the filter were fixed in 2% paraformaldehyde for 10 min and stained with 0.05% crystal violet for 15 min. For migration assay, the experiments were performed as above, except that cells were placed on the top of uncoated (Matrigel-free) inserts. Migrated and invaded cells were recorded under light microscopy after 14 h of incubation with or without the inhibitors.

2.9. Fractionation and membrane vesicles isolation

Tumors and cells plasma membranes were obtained by subcellular fractionation as described by Cotter et al. [25], with some modifications. Both were homogenized in medium containing: 50 mM MOPS-KOH (pH 7.2), 250 mM sucrose, 150 mM KCl, 150 mM EDTA, 1 mM DTT, 1 mM phenylmethylsulfonyl fluoride (PMSF), 3 mM benzamidine and bovine serum albumin (BSA) 0.03%. The solutions were maintained at 0–4 °C, at pH = 7.2. The tumors were previously homogenate and filtered using a Miracloth (MilliporeSigma) filtration material with a pore size of 22–25 μm, and culture cells were scraped. After that, both membrane vesicle preparation followed similar for tumors and cells, and were subjected to centrifugation (3000 ×*g*, 20 min). The pellet, which contains the densest homogenate fraction, was discarded and the supernatant was centrifuged at 100,000 ×*g* for 30 min. The resulting pellet was solubilized in the buffer, applied on a two-step sucrose gradient (46 and 25%, (*w*/*v*)) and centrifuged at 100,000 ×*g* for 3 h. The plasma membranes were obtained in the 46/25% sucrose interface. The protein content in the plasma membrane fraction was determined as described elsewhere [26], using BSA as a standard. The fraction containing the plasma membrane-enriched vesicles was used immediately or stored in liquid nitrogen for subsequent enzymatic analysis.

2.10. Enzyme activities

Plasma membranes-enriched vesicles (30 μg of protein) were added to the incubation medium containing 20 mM KCl, 2.5 mM $MgSO_4$, 12.5% sucrose, 20 mM MOPS-KOH, pH 7.2, and 2 μM ACMA (9-amino-6-cloro-2-methoxyacridine). Increasing concentrations of Myrtenal (25–100 μM) and 5 nM concanamycin A were used to evaluate its inhibitory effect, the membrane vesicles were preincubated with the inhibitors for 5 min. Proton transport was started by the addition of 1 mM ATP and the H^+ electrochemical gradient ($\Delta\mu H^+$) was monitored by measuring the fluorescence quenching of ACMA using a fluorescence spectrometer (Shimadzu RF-530 1PC). ATP hydrolysis was determined by measuring the amount of Pi released according to Fiske and Subbarow [27]. The reaction was stopped by adding ice-cold molybdate solution after 30 min of incubation, at 37 °C, in a medium containing: 1 mM ATP, 2.5 mM $MgSO_4$, Na_2MoO_4 and Hepes-Tris 10 mM pH 7.2. The V-type H^+-ATPase specific activity was calculated by the difference of ATP hydrolysis with and without 5 nM concanamycin A.

2.11. Proton fluxes (J_{H^+}) measurements in living tumor cells

Cell samples (1×10^6) were incubated in DMEM tissue culture in 34 mm round coverslips for 24 h. Thereafter, the J_{H^+} was measured at the cell surface using the non-invasive Scanning Ion-selective Electrode Technique (SIET) as described by Ramos et al. [28]. Living cells were incubated in DMEM, pH 7.0 at 37 °C, during 24 h, and H^+ fluxes at cell surface were monitored by an ion-selective 3D vibrating probe contained a hydrogen ionophore (H^+ ionophore I, Cocktail B, Sigma Aldrich®). The vibrating microelectrode was positioned near the cell surface and the net J_{H^+} were measured during 60 min, in the presence or absence of V-ATPase inhibitors, over an excursion distance of 15 μm to detect the H^+ specific μV difference and the data were also used to calculate the extracellular pH changes. Control measurements were performed at 300–500 μm distance away from the cells, and the background references were subtracted from measurements performed at the cells surface.

2.12. Metastatic dissemination assay

Male C57BL-6 mice, 6–8 weeks old, were maintained in pathogen-free conditions in laminar flow rooms under constant temperature and humidity and were fed with commercial standard food and water *ad libitum*. We used two approaches to analyze metastasis, in the first 1×10^6 B16F10 cells/mL in 50 μL DMEM were subcutaneously injected between the skin and cartilage on the dorsal side of the ear in order to evaluate lymph node metastatic dissemination, as described by Bobek et al. [29]. In the second approach the same number of cells were injected in the tail vein of the animals to evaluate the metastatic dissemination in lung [30]. The most effective non-toxic concentration for *in vivo* treatments was determined to be 15 mg/kg Myrtenal (Supplemental Fig. S1C). The tumor-bearing mice were randomly divided into 3 groups with 10 animals per group (untreated, DMSO and Myrtenal treated). Treatment was performed by intraperitoneal injection of 15 mg/kg Myrtenal, each 48 h, on alternating days for 21 days, tumor volumes were estimated by the formula: volume = 0.52. $(\text{width})^2$. Length [31]. Metastatic and control lungs or lymph nodes were removed and fixed in 10% neutral buffered formalin and stored at room temperature for histological processing and analyses. All procedures done with mice were approved by the Animal Ethics Committee of Universidade Estadual do Norte Fluminense Darcy Ribeiro (CEUA-1922012; Campos dos Goytacazes, Rio de Janeiro, Brazil).

2.13. Histological analysis

Mice from each experimental group were euthanized by CO_2 inhalation and their organs were removed and fixed with 10% neutral *p*-formaldehyde. All samples were processed according to standard histological techniques. Briefly, tissues were dehydrated in ascending concentrations of ethanol (70–100%) and embedded in paraffin using an automatic tissue processor (TP 1020, Leica, Germany). Then, 5 μm sections were stained with hematoxylin-eosin and tissue sections were

observed using a digital image analysis system coupled to a microscope (Zeiss Axioplan/Axiocam, Germany).

2.14. Statistical analysis

All experiments were performed at least four times, and the results were expressed as mean ± SD. GraphPad Prism 5 software was used for statistical analysis. Tukey test with Welch's correction and two-way-ANOVA Bonferroni posttest were used where appropriate. P values < .05 were considered statistically significant (* $P < .05$; ** $P < .01$; *** $P < .001$).

3. Results

3.1. Myrtenal inhibits the ATP hydrolysis, $\Delta\mu H^+$ and J_{H+} mediated by V-ATPase

Myrtenal effects on the hydrolytic activities of the V-ATPase and on the H^+ electrochemical gradient ($\Delta\mu H^+$) formed by this pump in plasma membrane-enriched vesicles were investigated by comparing its effect with that of concanamycin A, a well-known V-ATPase inhibitor (Fig. 1A-C). Myrtenal at the concentrations of 25 and 50 μM inhibited 20 and 40% of the V-ATPase activity, respectively, in poorly metastatic B16F0 cells (A), while the same range of concentration inhibited ~60% V-ATPase activity in highly metastatic B16F10 (B) and SkMel-5 cells (C). The $\Delta\mu H^+$ of the most metastatic melanoma cell lines was also inhibited by 100 μM Myrtenal (Fig. 1A-C). These data indicated that Myrtenal was almost as effective as 5 nM concanamycin A, the lowest concentration found to nearly fully inhibit the H^+ transport driven by the V-ATPase of the highest metastatic murine cell line B16F10; therefore, concanamycin A was used as a positive control of V-ATPase-inhibitory effects in the remaining experiments.

We also analyzed the proton fluxes (J_{H+}) at the surface of living B16F10 and B16F0 cells using the non-invasive scanning ion-selective electrode technique (SIET). The magnitude of the J_{H+} in B16F10 cells was greater than in B16F0 cells, correlating with the metastatic capacity of these melanoma cells (Fig. 1D). concanamycin A (5 nM) and Myrtenal (100 μM) significantly decreased J_{H+}. Myrtenal and concanamycin A also decreased J_{H+} in B16F10 cells exhibiting a time-dependent decrease and a complete inhibition after 20 min treatment (Fig. 1E). Analysis of the voltage difference across the cell membrane indicated that both V-ATPase inhibitors decreased the membrane energization (Fig. 1F-G) and induced alkalinization of extracellular microenvironment, which pH rose by about 0.4 pH unit from 7.0 to 7.4 in average (Fig. 1H).

3.2. Melanoma cell death induced by V-ATPase inhibitors

Cells stained with ethidium bromide and acridine orange were used to analyze the rates of cell death and the acidification of endocytic vesicles, respectively. The melanoma cell lines B16F0 and B16F10 and SkMel-5, exhibited a peripheral arrangement of acridine orange labeled vesicles (Fig. 2A). The analysis also revealed that all tumor cells underwent cell death when exposed for 12 h to 50 μM Myrtenal or 5 nM concanamycin A, while the vesicular acidity decrease started in all cell lines within the first 30 min of exposure (data not shown). After the treatment with Myrtenal, only a few scattered melanoma cells were labeled by ethidium bromide, indicative of low levels of necrosis. However, clear features of apoptosis were observed, such as chromatin condensation and fragmentation of pyknotic nuclei in B16F10, B16F0 and SkMel-5. For human SkMel-5 cell line, we also observed further apoptotic patterns, such as nuclear shrinkage and membrane blebbing (Fig. 2A). All cell lines treated with Myrtenal also showed signals of cell death quite like those induced by concanamycin A. However, necrotic cells were much more prevalent following concanamycin A treatment, as indicated by ethidium bromide staining (Fig. 2A). The ultrastructural analyses also revealed apoptotic features in all cell lines, varying with the metastatic potential of the cell line (Fig. 2B). The highly metastatic B16F10 mice melanoma cells presented numerous cellular micro-projections characteristic of cells with high migratory capacity, but such cell adhesion structures decreased with Myrtenal treatment. The chromatin condensation was observed in all cell lines at higher Myrtenal concentrations (> 100 μM). Moreover, the human SkMel-5 cell line was the most responsive to Myrtenal treatment, accumulating many multivesicular bodies and vacuoles (Fig. 2B), apoptotic features previously described to be a typical mode of cell death induced by V-ATPase inhibitors [16].

Flow cytometry assays were performed to evaluate the rates of phosphatidylserine exposure on cell subsurface to identify early (Annexin$^+$, PI$^-$) and late apoptotic cells (Annexin$^+$, PI$^+$). Data were expressed as a percentage of total apoptotic cells (early plus late apoptosis). Similar results were obtained when cells were treated with either Myrtenal or concanamycin A in murine melanoma B16F0 and B16F10 cells, but for the highly metastatic human cell line SkMel-5, approximately, 80% and 50% of programmed cell death was found under treatment with Myrtenal and concanamycin, respectively. In general, Myrtenal treatment caused a 5-fold increase in the number of cells death in SkMel-5 cells (Fig. 3D), 4-fold increase in B16F0 and B16F10 cells (Fig. 3B-D) and only 2-fold in non-cancer J774 A_1 cells (Supplemental Fig. S2B). Similar levels of apoptosis were observed by using the specific V-ATPase inhibitor, however, the number of necrotic cells was significantly higher under concanamycin effect (Supp Fig. 2B; C). Treatment of highly metastatic tumor cells (SkMel-5, B16F10) with 100–200 μM Myrtenal for 24 h significantly decreased (40–50%) cell viability, in contrast to the slight effect (10–30%) on the low metastatic B16F0 cells (Supplemental Fig. S1B) and non-tumor J774 A_1 cells (Supplemental Fig. S2A).

3.3. Myrtenal decreases cell migration and invasion of melanoma cells

To further investigate the Myrtenal's therapeutic potential, we examined its effect on cell migration. We found that B16F10 cells completely covered the wound-scratch after 24 h (Fig. 4A), much faster than B16F0 cells (data not shown), indicative of a higher migratory ability closely related to the aggressive metastatic potential of B16F10. The addition of 5–10 μM Myrtenal resulted in a concentration-dependent decrease of cell migration almost completely abolishing the migratory activity at the higher concentration quite similar to the effect induced by the V-ATPase inhibitory control related to the effect induced by 5 nM concanamycin A (Fig. 4B). Transwell migration assays confirmed these results indicating that cell migration is faster in B16F10 than in B16F0 melanoma cells (Fig. 4C, E) and that both Myrtenal and concanamycin A inhibited cell invasion of melanoma cells *in vitro* (Fig. 4 D, F).

By using a syngeneic model of spontaneous metastatic B16 murine melanoma [29] to determine the significance of these findings *in vivo*, we induced tumors in mouse by injection of B16F10 cells into the mouse ear or into the tail vein. This approach allowed us to evaluate metastatic dissemination in the mandibular lymph nodes and lungs, respectively. To investigate the potential anti-cancer effect of Myrtenal, we injected intraperitonial 15 mg/kg Myrtenal for 21 days. Fig. 5A illustrates typical untreated mouse's metastatic lymph nodes with highly affected regions, exhibiting loss of capsule integrity, melanin accumulation spots and necrosis. Mice treated with Myrtenal exhibited less metastasis, preservation of the capsule integrity and less tissue damage. It was also possible to observe remarkable areas of tumor regression in the lungs of mice treated with Myrtenal, indicating its potential to treat cancer metastasis (Figs. 5B and 6C).

Myrtenal treatment decreased tumor growth and caused a six-fold reduction of tumor nodules, compared to the control mice where we usually found about two hundred pulmonary metastatic nodules (Fig. 6C). Non-treated mice developed rapidly growing metastatic tumors (Fig. 6A and B). Importantly, Myrtenal treatment for 21 days

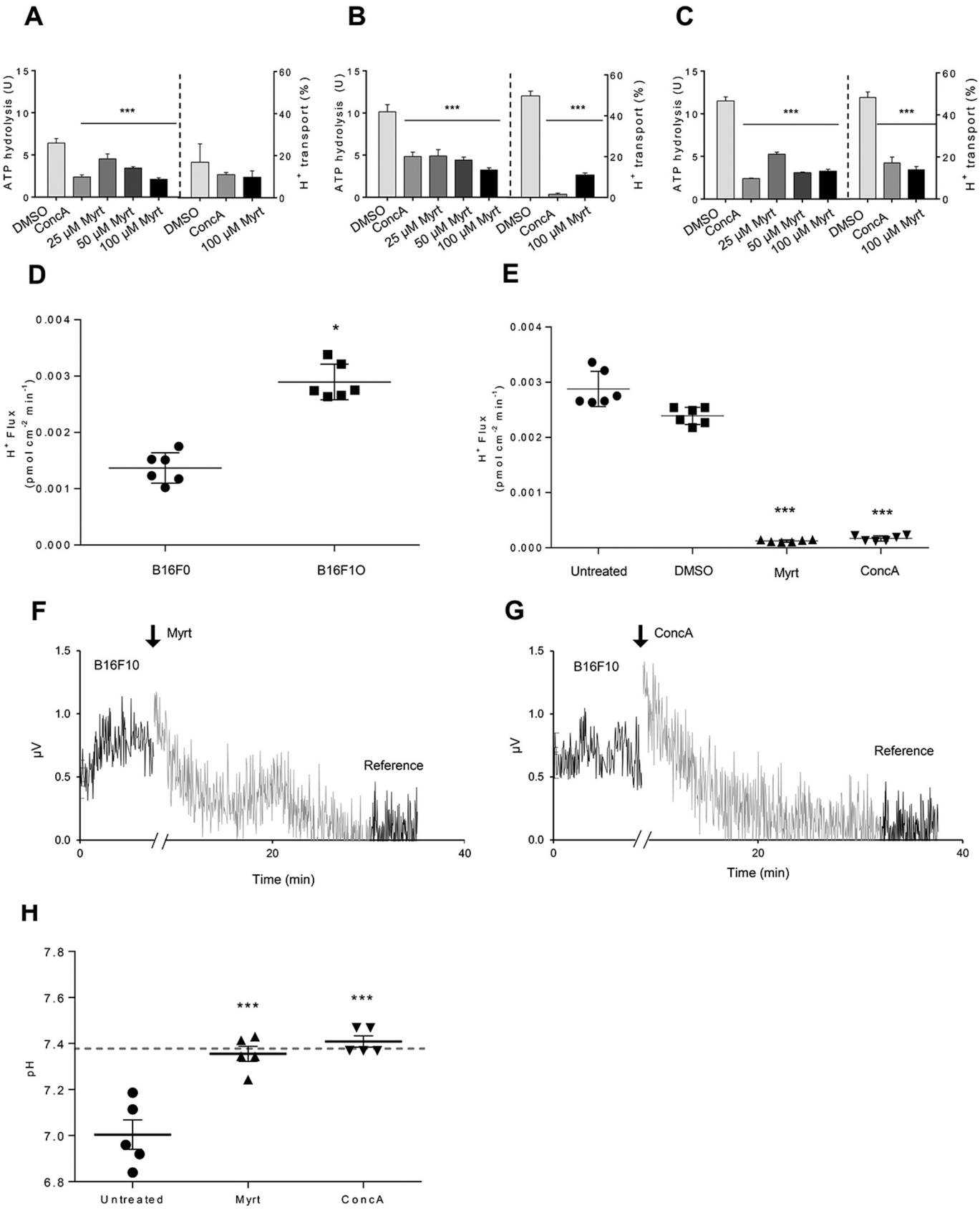

Fig. 1. Effects of Myrtenal on V-ATPase activity and H^+ flux. V-ATPase concanamycin-sensitive hydrolytic activity U = µmolPi.mg^{-1}.min^{-1} and proton pumping were determined in plasma membrane-enriched vesicles isolated from B16F0 (A), B16F10 (B) and SkMel-5(C) cell lines in the presence of Myrtenal. Proton flux over time in culture cells were measured using non-invasive Scanning Ion-selective Electrode Technique in live B16F0 and B16F10 cells treated with DMSO (D), and B16F10 were evaluated with 100 µM Myrtenal and 5 nM concanamycin A (E), and a representative profile is shown for each case. Voltage differences across the B16F10 cell membrane were measured in the presence of Myrtenal (F) or concanamycin A (G), and extracellular pH was quantified in B16F10 after 30 min of treatment Statistically significant differences were determined using 2-way ANOVA followed by a Bonferroni post-hoc test. $N = 5$, $^*p < .05$, $^{**}p < .01$, $^{***}p < .001$.

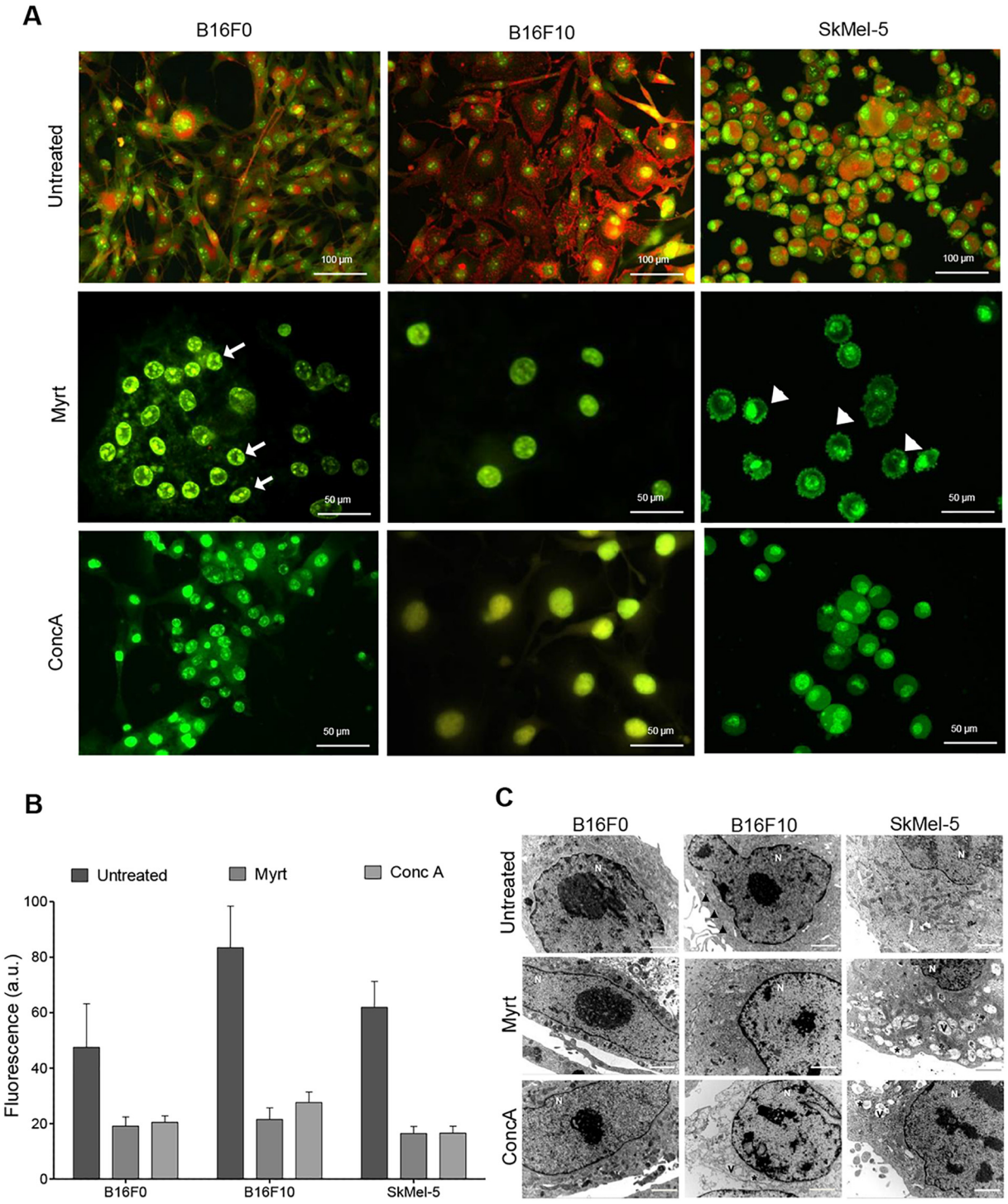

Fig. 2. Myrtenal reduces acidification and promotes cell death in melanoma cells. (A and B) Dual acridine orange/ethidium bromide fluorescence staining of cells after incubation with 50 µM Myrtenal and 5 nM concanamycin A for 12 h, and quantification of cell fluorescence. Arrows indicate the pyknotic nuclei and arrowheads indicate the membrane blebbing in apoptotic cells. (C) Cellular morphological changes in the initial stages of cell death after incubation with 100 µM Myrtenal and 5 nM concanamycin A for 18 h, as revealed by transmission electron microscopy. Arrowheads indicate the migratory microprojections characteristic of highly metastatic B16F10 cells. Apoptotic features such as nuclear condensation, vacuolization and membrane blebs following drug treatment are clearly detected mainly in the human cell line SkMel-5. Abbreviations: V, vacuoles, *n*, nucleus; *, multivesucular bodies. *** $p < .001$. Scale bars: 500 nm (C).

significantly improved survival (Fig. 6D). Enzymatic analysis of plasma membranes isolated from tumors induced in mice indicated that Myrtenal inhibits 50% of the concanamycin-sensitive ATP hydrolysis when compared to plasma membranes of tumors-induced in untreated mice (Fig. 6E and F). Altogether, these data indicate that Myrtenal is a potential anti-cancer chemotherapeutic drug to halt metastatic dissemination of highly aggressive tumor cells.

4. Discussion

Most anti-cancer drugs can be classified into two groups, those which are composed of inhibitors of the initiation phase of

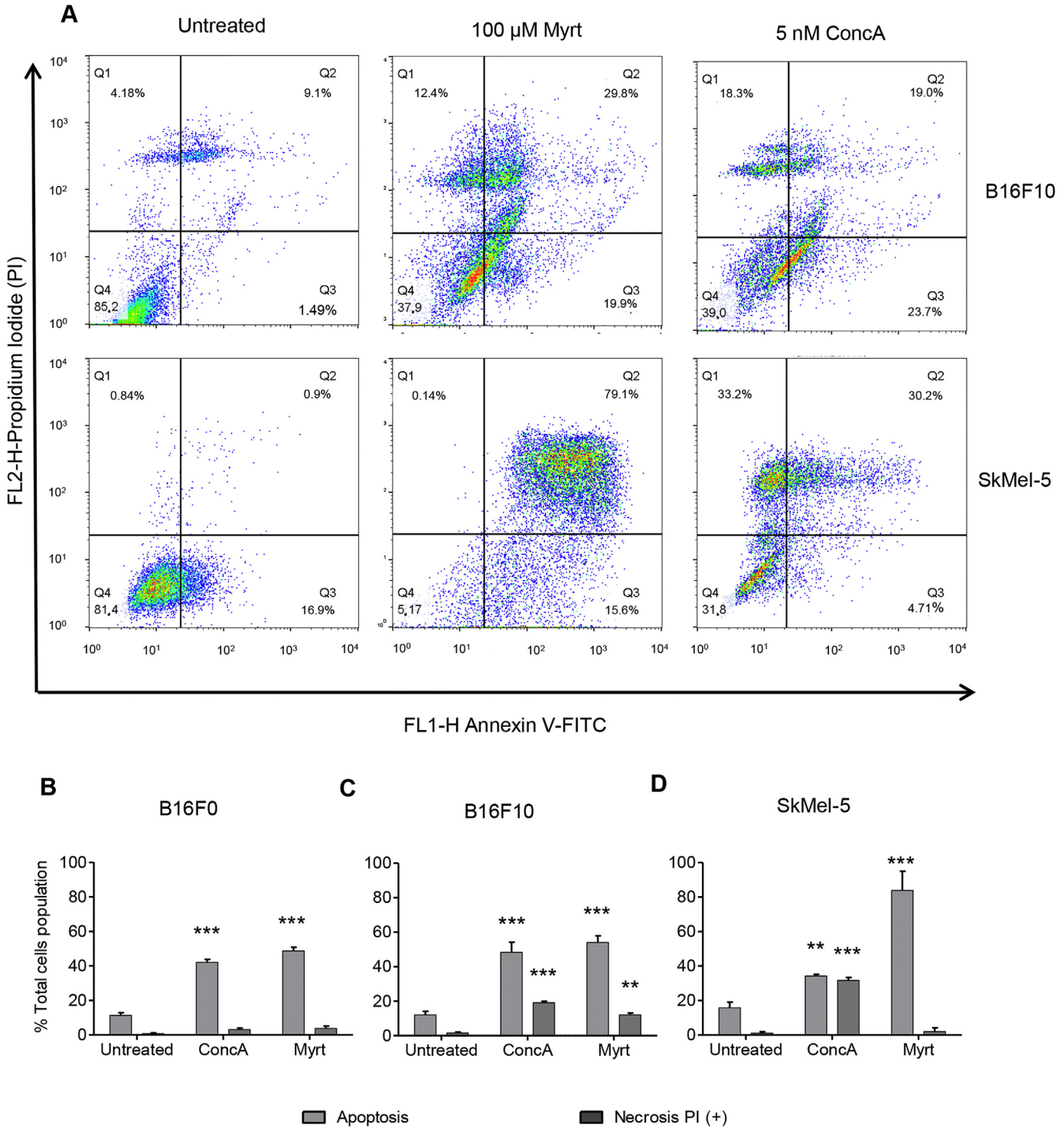

Fig. 3. Myrtenal-induced apoptosis in melanoma cells. The cells were exposed to 100 μM Myrtenal and 5 nM concanamycin A for 24 h and stained with FITC-Annexin V and propidium iodide (PI). The apoptotic cells as detected by flow cytometry analysis: (A) Representative dot/density plots of B16F10 and SkMel-5 cells are shown. Annexin V^+/PI^- and Annexin V^+/PI^+ cells were designed as early and late stage of the apoptotic process, respectively. Flow cytometry data are presented as the percentage of apoptotic and necrotic cells for B16F0 (B), B16F10 (C), SkMel-5 (D). Values are means ± SD ($n = 4$). Statistically significant differences were determined using 2-way ANOVA with Bonferroni's post-test (*$p < .05$, **$p < .01$, ***$p < .001$).

carcinogenesis process, and those that inhibit cell proliferation and tumor progression [31]. Cancer suppressing agents capable of activating programmed cell death and prevent metastasis deserve special attention in drug discovery efforts, since they can be effective before and after the onset of the disease [32]. It has been shown that specific V-ATPase inhibitors, such as bafilomycin and concanamycin, induce apoptosis in several types of cancer [33–36]; however, such macrolide antibiotics have significant toxicity that precludes their usefulness in the clinic [37]. Recently, less toxic proton pump inhibitors have increasingly been found and demonstrated similar effects in eliciting programmed cancer cell death [38,39]. Here, we reported that the monoterpene Myrtenal, considered nontoxic and commercialized as a

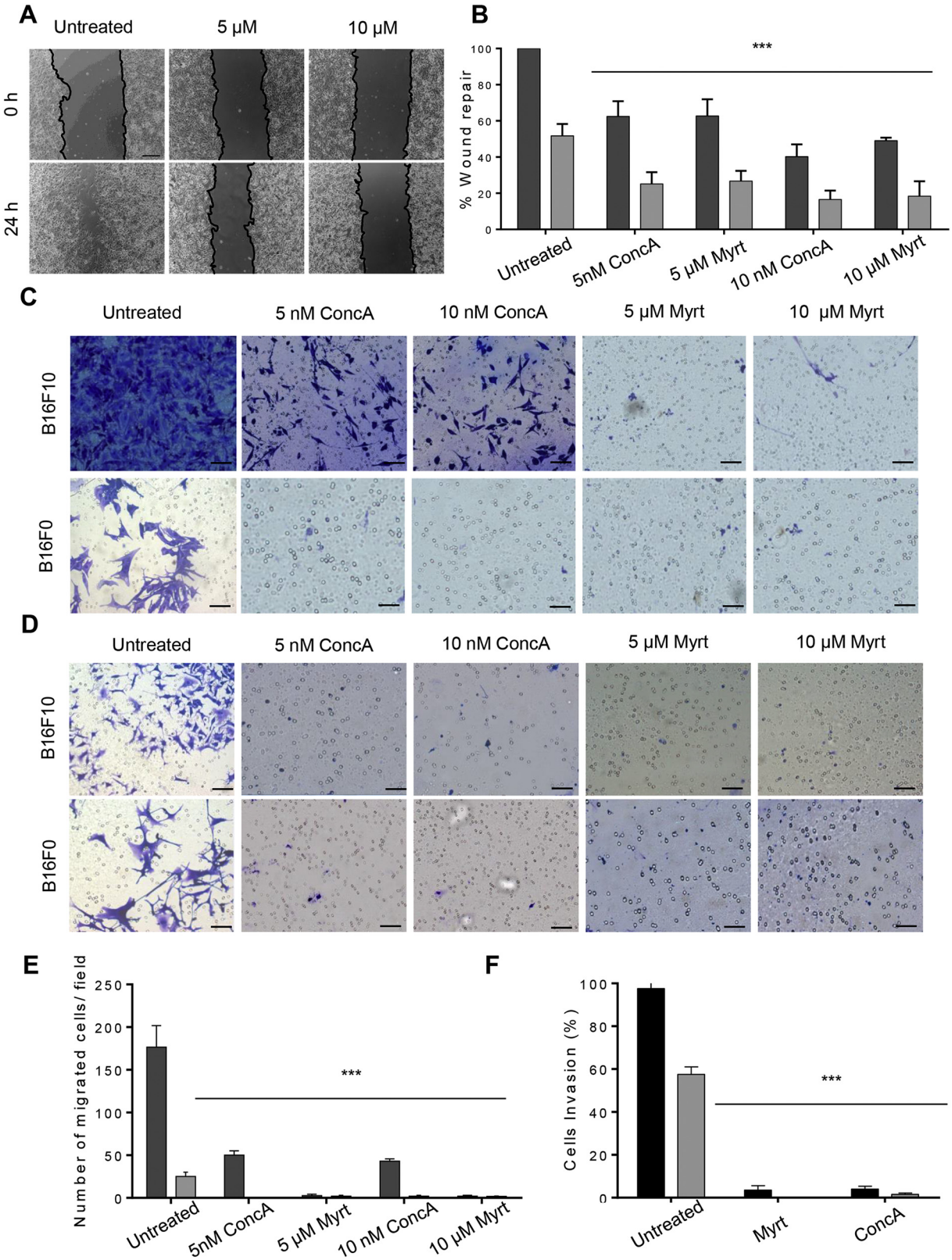

Fig. 4. Myrtenal decreases invasion and migration of melanoma cells (A) Cell migration of B16F10 cells was evaluated under microscope by wound-healing assay in presence or absence of Myrtenal (5 and 10 μM). Representative images of cells at 0 h and 24 h after scratch are shown. (B) Quantification of wound closure in B16F10 and B16F0 cell lines in the presence of Myrtenal (5 and 10 μM) and 5 nM concanamycin A. Note that in the absence of Myrtenal (control treatment) B16F10 cells exhibited higher migratory rates l than B16F0 cells. Transwell chamber assay comparing B16F0 and B16F10 cell migration (C and E) and invasion (D and F) in 5 or 10 nM concanamycin A, and 5 or 10 μM Myrtenal. Representative images of the bottom of the transwell migration (C) and invasion assays (D) are shown. Values are means ± SD ($n = 3$). Statistically significant differences were determined using 2-way ANOVA with Bonferroni's post-test (***$p < .001$).

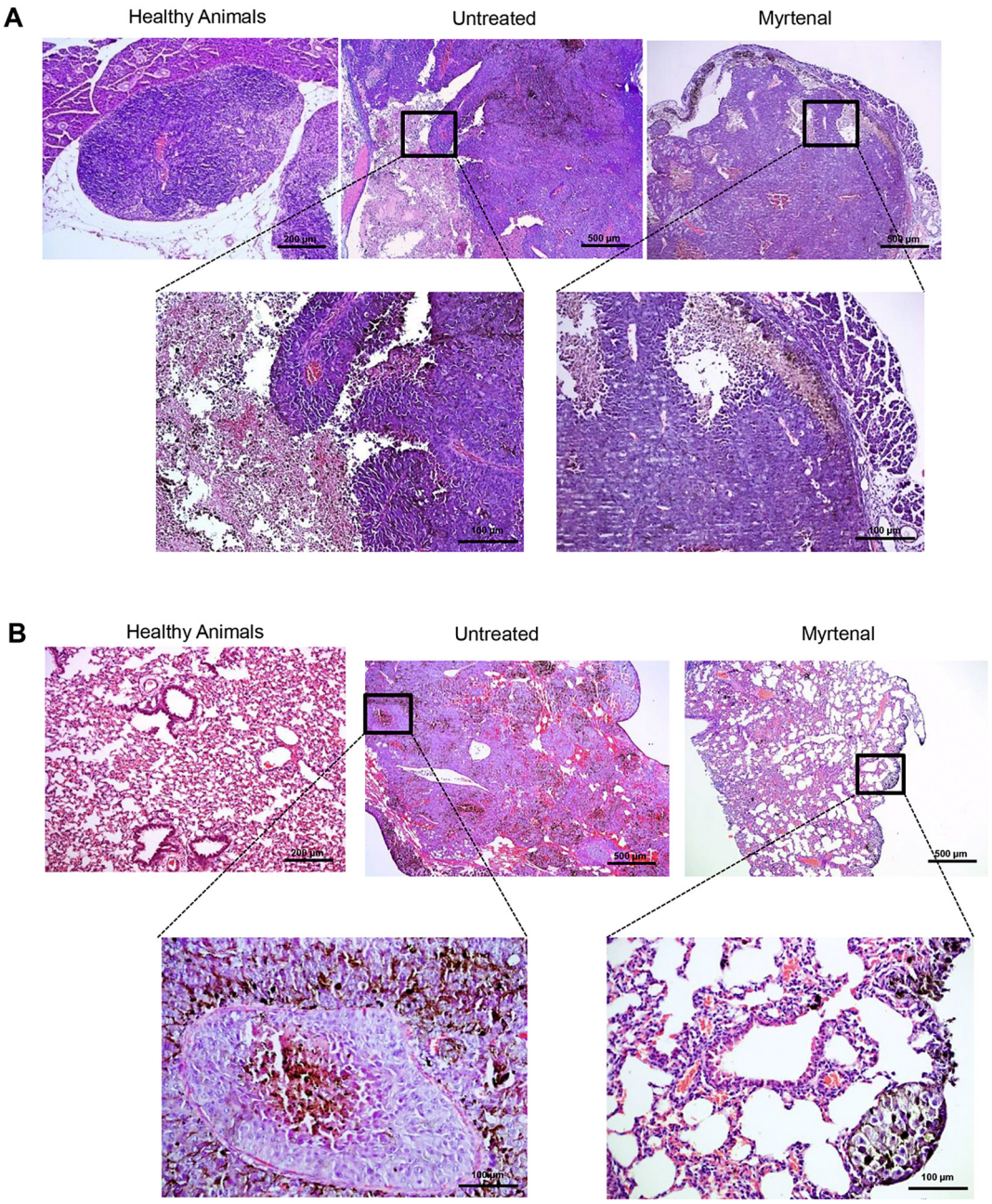

Fig. 5. Histological analysis of the Myrtenal effect on metastatic melanoma. Tumors were induced by injection of B16F10 cells into the mouse ear or in tail vein and the metastasis was analyzed in the lymph node (A) or in lungs (B), respectively. Metastasis induced by B16F10 cells was decreased by treatment with 15 mg/kg Myrtenal for 21 days. Scale bars: 500 µm (A) and 100 µm (B).

food additive, has a clear anti-melanoma activity mediated by inhibition of V-ATPases, sharply decreasing metastasis *in vivo*. Our data provide evidences for the capacity of Myrtenal to trigger cell death in melanoma cells with a higher efficiency in highly metastatic murine B16F10 and human SkMel-5 melanoma cell lines (Figs. 2, 3 and Supplemental Fig. S1B). Minor cytotoxic effects were observed in the low metastatic B16F0 cell line (Fig. 3B-D) as well as in non-cancer J774 A_1 cells (Supplemental Fig. S2B), which showed very low levels of necrosis and higher cell viability upon Myrtenal treatment. Yet, this monoterpene demonstrated some apoptotic effect even on immortalized cells of the non-cancer model J774 A_1 (~30%), whereas apoptosis levels in tumoral cells varied from 40 to 80% in low metastatic B16F0 and highly metastatic SkMel-5 cell lines, respectively. These findings are especially important considering that loss of apoptosis and acquisition of a multidrug resistance phenotype represent some of the main factors related to melanoma progression and metastasis [40], and melanoma has been described as one of the cancers of the highest resistance to apoptosis-inducing agents [41]. Indeed, pharmacological inhibition of V-ATPase reversed resistance of breast cancer to chemotherapy [42], and this proton pump has proved to be involved in the acquisition of the multidrug resistance phenotype [10,43].

Cancer selectivity and minimal toxicity are highly desired but rarely achieved properties of anticancer agents [31]. In this regard, Myrtenal exhibited a quite higher cytotoxicity toward highly metastatic melanoma cells in comparison to the less aggressive melanoma cell line and non-cancer J774 cells, which maintained higher levels of cell viability at high Myrtenal concentrations. It is worth noting that no detectable systemic adverse effects were induced by the Myrtenal on *in vivo* treatment in the mouse model. Furthermore, long-term use as flavor/food additive of this monoterpene all over the world has proven it to be

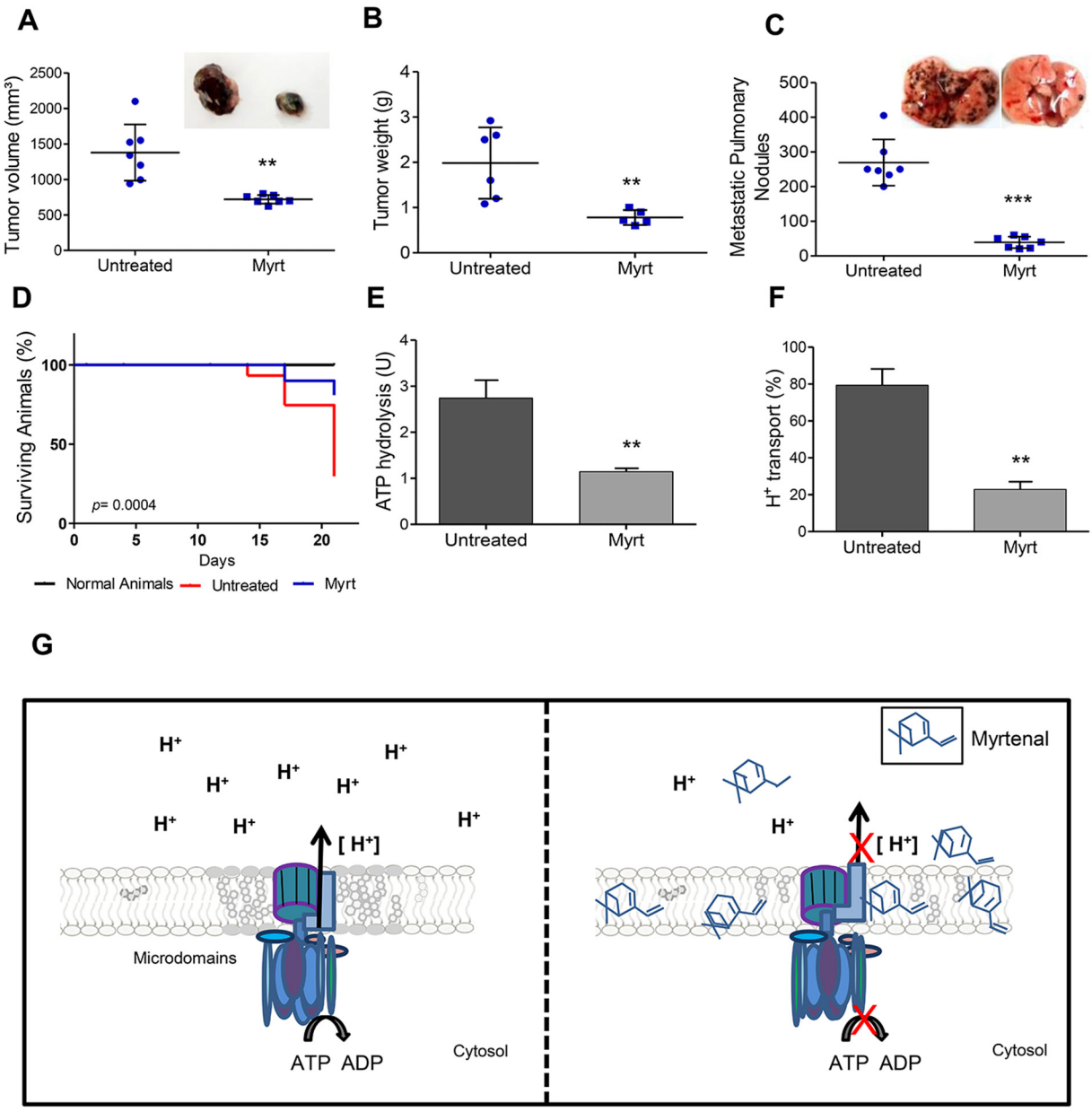

Fig. 6. Anti-metastatic activity of Myrtenal related to the V-ATPase inhibition. Induced melanoma in lymph node tumors, volume (A) and weight (B), and number of nodules in metastatic lungs (C) from mice treated (right) or not (left) with 15 mg/kg Myrtenal by intraperitoneal injection each 48 h for 21 days. Primary tumors weight and volume (A and B) and animal survival rates (D) were determined on the 21th days after tumor induction using Log-rank (Mantel-Cox) Test. Tumors were removed and used for isolation of plasma membranes-enriched vesicles by cell fractionation as described in Materials and Methods; (E) concanamycin-sensitive V-ATPase hydrolytic activity U = μmolPi.mg^{-1}.min^{-1} and initial velocity of the H^+ transport in cell membranes of primary tumors (F) were determined in mice upon Myrtenal treatment compared to untreated ones. (G) A proposed model for the Myrtenal mechanism of action by interacting with membrane microdomains and inactivating the V-ATPase. Values are means ± SD (n = 4). *$p < .05$, **$p < .01$,***$p < .001$ (unpaired Student's t-test with Welch's correction) represent statistically significant differences from controls.

relatively safe, especially when compared with most of the commercially available chemotherapeutics.

The efficacy of Myrtenal to induce V-ATPase inhibition in metastatic melanoma cells was associated with a decrease in the H^+ fluxes to the extracellular matrix (Fig. 1), and a decreased intravesicular acidification (Fig. 2), therefore disrupting V-ATPase-dependent pH signatures related to tumor-proliferative activity and impairing metastasis (Fig. 6). Myrtenal elicited an almost complete inhibition of the acidic compartments as determined by acridine orange in all cells, however, the effect was more pronounced in highly metastatic cells (Fig. 2A). Myrtenal inhibitory activity was found as early as after 1 h of treatment, when clear apoptosis signals in B16F10 cells were already detectable, associated with a decrease in vesicular acidification, as determined by acridine orange. These results are in agreement with data on other natural compound, diphylline, which also inhibited V-ATPase and promoted apoptosis in gastric adenocarcinoma cell lines [44]. One of the first steps in apoptosis is the translocation of phosphatidylserine from the inner leaflet to the outer leaflet of the plasma membrane [45,46]. After 24 h of Myrtenal treatment, human melanoma (SkMel-5) and metastatic murine melanoma (B16F10 and B16F0) cells exhibited a significant decrease in cell viability.

The effectiveness of such a mechanism of action is in line with the notion that not only the acidification of the extracellular microenvironment, but also other V-ATPase-dependent pH signatures play

key roles in tumor malignancy and metastatic potential [19]. Indeed, in addition to the induction of apoptosis, our study also shows that at lower concentrations (5–10 μM) Myrtenal decreased cell migration and cell invasion *in vitro* and its efficacy in reducing tumor growth and metastatic dissemination *in vivo* was demonstrated. The reduction of migration and invasion of tumor cells was also described for other V-ATPase inhibitors, such as Nik-12,192 [47] and bafilomycin [13], in non-small lung and breast cancer cells, respectively. *In vitro*, we have already shown that V-ATPase inhibition by membrane cholesterol depletion decreased melanoma cell migration and invasiveness [19]. Therefore, it was not surprising to find a significant decrease in metastatic dissemination in the lymph nodes and lungs following Myrtenal treatment *in vivo*. In addition, the body weight of treated mice remained stable and the survival rates were significantly improved when compared to untreated mice (Figs. 5-6). The ATP hydrolysis catalyzed by the V-ATPase in plasma membranes isolated from tumors of Myrtenal-treated animals was significantly reduced (Fig. 6E and F), reinforcing that Myrtenal effects in decreasing metastatic dissemination should be also related to inhibition of V-ATPase *in vivo*.

In regard to the Myrtenal mode of action, an analogous effect to that we have recently reported [19] on destabilization of membrane microdomains as disturbing the activity of intrinsic proteins like the V-ATPase should be expected, since monoterpenes are highly hydrophobic substances covering a wide spectrum of bioactivities with a membrane interaction as a common feature [48]. In agreement, metabolomics data confirmed the intramembrane localization of Myrtenal [3]. Moreover, like other monoterpenes it could interact with cholesterol [49] and induce changes in the membrane structural organization and surface electrostatics disrupting functional rafts of which the V-ATPase activity was shown to depend [19]. At higher concentrations (100 μM) Myrtenal could induce apoptosis due to the collapse of the tumor acidification by a mechanism of action typical of pharmacological V-type proton pumps inhibition [16]. The V-ATPase inhibition along with the collapse of the secondary transport system of nutrients would elicit an acute energy stress, which in turn would induce cellular autophagy among other anoxia related factors. These processes are succeeded by a shutdown of energy-consuming processes trying to escape cell death. But prolonged activation of these processes would eventually lead to apoptosis induction, especially when the electrochemical gradient of H^+ is disturbed in plasma membrane as well as in endomembrane vesicles as is the case of Myrtenal treatment here described (Fig. 1 and Fig. 2). On the other hand, at lower concentrations (5–10 μM) Myrtenal would inhibit cell migration and metastatic dissemination by disrupting V-ATPase-dependent pH signatures [19], which modulate a myriad of metastasis related processes, underlying cytoskeleton reorganizing, vesicles traffic, and the functionality of adhesion structures. Because of the complex interrelation of the migration and invasiveness parameters to be assessed along with specific electrochemical H^+ gradients oscillations in plasma membranes and endomembranes, this mode of action drawn above requires further mechanistic investigations. A proposed model for the Myrtenal mechanism of action by interacting with lipid membrane microdomains and inactivating the V-ATPase is shown in Fig. 6G.

In conclusion, mechanistically compelling evidences are provided establishing that Myrtenal toxicity and anti-melanoma effects are related to inhibition of V-ATPases expressed in the tumors cells and impaired J_{H+}, which in turn leads to apoptosis induction and decreased cell migration and invasion, and impaired metastatic dissemination. The understanding of the mechanism of toxicity underlying the Myrtenal anti-cancer properties opens a new avenue to explore its pharmacological potential and may be also instrumental for assessment of putative adverse influences on normal cells upon accidental exposure to toxic concentrations of a monoterpene widely utilized in food industry. Moreover, Myrtenal has proved to be a potential chemotherapeutic agent endowed with the capacity to halt animals/human melanoma metastasis and thus should be considered for further evaluation in clinical trials.

Supplementary data to this article can be found online at https://doi.org/10.1016/j.bbagen.2018.09.006.

Acknowledgements

We are grateful to Dr. Jean-Jacques Lebrun for the critical reading of the manuscript. This work was supported by CNPq (Conselho Nacional de Desenvolvimento Científico e Tecnológico) and FAPERJ (Fundação de Amparo à Pesquisa do Estado do Rio de Janeiro). BXM and GAC received a PhD fellowship from UENF, RFA and JMS from CAPES (Coordenação de Aperfeiçoamento de Pessoal de Nível Superior – Finance Code 001), and SBF from CAPES and FAPERJ.

Conflict of interest

The authors declare that they have no conflict of interest.

References

[1] F. Bakkali, S. Averbeck, D. Averbeck, M. Idaomar, Biological effects of essential oils - a review, Food Chem. Toxicol. 46 (2008) 446–475, https://doi.org/10.1016/j.fct.2007.09.106.
[2] J.M.P. Ferreira De Oliveira, A.R. Pacheco, L. Coutinho, H. Oliveira, S. Pinho, L. Almeida, E. Fernandes, C. Santos, Combination of etoposide and fisetin results in anti-cancer efficiency against osteosarcoma cell models, Arch. Toxicol. 92 (2017) 1205–1214, https://doi.org/10.1007/s00204-017-2146-z.
[3] National Center for Biotechnology Information, PubChem Compound Database CID = 61130, https://pubchem.ncbi.nlm.nih.gov/compound/Myrtenal#section=Top, (2018) , Accessed date: 15 January 2018.
[4] C.S. Pereira, J.P. Guedes, M. Gonçalves, L. Loureiro, L. Castro, H. Gerós, L.R. Rodrigues, M. Côrte-Real, Lactoferrin selectively triggers apoptosis in highly metastatic breast cancer cells through inhibition of plasmalemmal V-H^+-ATPase, Oncotarget 7 (2016) 62144–62158, https://doi.org/10.18632/oncotarget.11394.
[5] J. Capecci, M. Forgac, The function of vacuolar ATPase (V-ATPase) a subunit isoforms in invasiveness of MCF10a and MCF10CA1a human breast cancer cells, J. Biol. Chem. 288 (2013) 32731–32741, https://doi.org/10.1074/jbc.M113.503771.
[6] J. Ferlay, I. Soerjomataram, R. Dikshit, S. Eser, C. Mathers, M. Rebelo, D.M. Parkin, D. Forman, F. Bray, Cancer incidence and mortality worldwide: sources, methods and major patterns in GLOBOCAN 2012, Int. J. Cancer 136 (2015) E359–E386, https://doi.org/10.1002/ijc.29210.
[7] R.M. Webster, S.E. Mentzer, The malignant melanoma landscape, Nat. Rev. Drug Discov. 13 (2014) 491–492, https://doi.org/10.1038/nrd4326.
[8] E. Orouji, A. Orouji, T. Gaiser, L. Larribere, C. Gebhardt, J. Utikal, MAP kinase pathway gene copy alterations in NRAS/BRAF wild-type advanced melanoma, Int. J. Cancer 138 (2016) 2257–2262, https://doi.org/10.1002/ijc.29970.
[9] O. Warburg, On the origin of cancer cells, Science 123 (1956) 309–314, https://doi.org/10.1126/science.123.3191.309.
[10] S. Fais, A nonmain stream approach against cancer, J Enzyme Inhib Med Chem. 31 (2016) 882–889, https://doi.org/10.3109/14756366.2016.1156105.
[11] R. Martinez-Zaguilán, R.M. Lynch, G.M. Martinez, R.J. Gillies, Vacuolar-type H^+-ATPase are functionally expressed in plasma membranes of human tumor cells, Am. J. Phys. 265 (1993) C1015–C1029, https://doi.org/10.1152/ajpcell.1993.265.4.C1015.
[12] R. Martínez-Zaguilán, E.A. Seftor, R.E. Seftor, Y.W. Chu, R.J. Gillies, M.J. Hendrix, Acidic pH enhances the invasive behavior of human melanoma cells, Clin. Exp. Metastasis 14 (1996) 176–186, https://doi.org/10.1007/BF00121214.
[13] S.R. Sennoune, K. Bakunts, G.M. Martınez, J.L. Chua-Tuan, Y. Kebir, M.N. Attaya, R. Martınez-Zaguilan, Vacuolar H^+-ATPase in human breast cancer cells with distinct metastatic potential: distribution and functional activity, Am. J. Phys. Cell Phys. 286 (2004) 1443–1452, https://doi.org/10.1152/ajpcell.00407.2003.
[14] K. Cotter, L. Stranky, C. McGuire, M. Forgac, Recent insights into the structure, regulation, and function of the V-ATPase, Trends Biochem. Sci. 40 (2015) 611–622, https://doi.org/10.1016/j.tibs.2015.08.005.
[15] L. Stransky, K. Cotter, M. Forgac, The function of V-ATPase in cancer, Physiol. Rev. 96 (2016) 1071–1091, https://doi.org/10.1152/physrev.00035.2015.
[16] K. von Schwarzenberq, R.M. Wiedmann, P. Oak, S. Schulz, H. Zischka, G. Wanner, T. Efferth, D. Trauner, A.M. Vollmar, Mode of cell death induction by pharmacological vacuolar H^+-ATPase (V-ATPase) inhibition, J. Biol. Chem. 288 (2013) 385–1396, https://doi.org/10.1074/jbc.M112.412007.
[17] D. Lagadic-Gossmann, L. Huc, V. Lecureur, Alterations of intracellular pH homeostasis in apoptosis: origins and roles, ell Death Differ. 11 (2004) 953–961, https://doi.org/10.1038/sj.cdd.4401466.
[18] J.M. Santos, R. Martínez-Zaguilán, A.R. Façanha, F. Hussain, S.R. Sennoune, Vacuolar H^+-ATPase in the nuclear membranes regulates nucleo-cytosolic proton gradients, Am. J. Phys. Cell Phys. (4) (2016) C547–C558, https://doi.org/10.1152/ajpcell.00019.2016.
[19] G.A. Costa, S.B. de Souza, L.R. da Silva, L. A. Okorokov, A.C.V. Arnholdt, A.L. Okorokova-Façanha, A.R. Facanha. Tumor cell cholesterol depletion and V-ATPase inhibition as an inhibitory mechanism to prevent cell migration and invasiveness in

melanoma. Biochim. Biophys. Acta 1862 (2018) 684–691. Doi: doi.org/https://doi.org/10.1016/j.bbagen.2017.12.006.
[20] K.C. Jefferies, D.J. Cipriano, M. Forgac, Funcion, structure and regulation of the vacuolar (H^+)-ATPases, Arch Biochim Biophys. 476 (2008) 33–42, https://doi.org/10.1016/j.abb.2008.03.025.
[21] T. Mosmann, Rapid colorimetric assay for cellular growth and survival: application to proliferation and cytotoxicity assays, J. Immunol. Methods 65 (1983) 55–63, https://doi.org/10.1016/0022-1759(83)90303-4.
[22] S. Kasibhatla, G.P. Amarante-Mendes, D. Finucane, T. Brunner, E. Bossy-Wetzel, D.R. Green, Acridine orange/ethidium bromide (AO/EB) staining to detect apoptosis, CSH Protoc (2006), https://doi.org/10.1101/pdb.prot4493.
[23] T. Kirkegaard, A.G. Roth, N.H.T. Petersen, A.K. Mahalka, O.D. Olsen, I. Moilanen, A. Zylicz, J. Knudsen, K. Sandhoff, C. Arenz, P.K.J. Kinnunen, J. Nylandsted, M. Jaattela, Hsp70 stabilizes lysosomes and reverts Niemann-pick disease-associated lysosomal pathology, Nature Lett. 463 (2010) 549–554, https://doi.org/10.1038/nature08710.
[24] M.L. Marino, S. Fais, M. Djavaheri-Mergny, A. Villa, S. Meschini, F. Lozupone, G. Venturi, P. Della Mina, S. Pattingre, L. Rivoltini, P. Codgno, A. De Milito, Proton pump inhibition induces autophagy as a survival mechanism following oxidative stress in human melanoma cells, Cell Death Dis. 1 (2010) e87, https://doi.org/10.1038/cddis.2010.67.
[25] K. Cotter, J. Capecci, S. Sennoune, M. Huss, M. Maier, R. Martinez-Zaguilan, M. Forgac, Activity of plasma membrane V-ATPase is critical for the invasion of MDA-MB231 breast cancer cells, J. Biol. Chem. 290 (2015) 3680–3692, https://doi.org/10.1074/jbc.M114.611210.
[26] M.M. Bradford, A rapid and sensitive method for quantitation of microgram quantities of protein utilizing the principle of protein-dye-binding, Anal. Biochem. 72 (1976) 248–254, https://doi.org/10.1016/0003-2697(76)90527-3.
[27] C.H. Fiske, Y. Subbarow, The colorimetric determination of phosphorus, J. Biol. Chem. 66 (1925) 375–400.
[28] A.C. Ramos, A.R. Façanha, J.A. Feijó, Proton H^+ flux signature for the presymbiotic development of the arbuscular mycorrhizal fungi, New Phytol. 178 (2008) 177–188, https://doi.org/10.1111/j.1469-8137.2007.02344.x.
[29] V. Bobek, K. Kolostova, D. Pinterova, G. Kacprzak, J. Adamiak, J. Kolodziej, M. Boubelik, M. Kubecova, R.M. Hoffman, A clinically relevant syngeneic model of spontaneous, highly metastatic B16 mouse melanoma, Anticancer Res. 12 (2010) 4799–4803.
[30] L.G. Menon, R. Kuttan, G. Kuttan, Inhibition of lung metastasis in mice induced by B16F10 melanoma cells by polyphenolic compounds, Cancer Lett. 95 (1995) 221–225, https://doi.org/10.1016/0304-3835(95)03887-3.
[31] N.H.T. Petersen, O.D. Olsen, L. Groth-Pedersen, A.M. Ellegaard, M. Bilgin, S. Redmer, M.S. Ostenfeld, D. Ulanet, T.H. Dovmark, A. Lonborg, S.D. Vindelov, D. Hanaham, C. Arenz, C.S. Ejsing, T. Kirkeggaard, M. Rohde, J. Nylandsted, M. Jaattela, Transformation-Associated changes in sphingolipid metabolism sensitize cells to lysosomal cell death induced by inhibitors of acid sphingomyelinase, Cancer Cell 24 (2013) 379–393, https://doi.org/10.1016/j.ccr.2013.08.003.
[32] S. Nobili, D. Lippi, E. Witort, M. Donnini, L. Bausi, E. Mini, S. Capaccioli, Natural compounds for cancer treatment and prevention, Pharmacol. Res. 59 (2009) 365–378, https://doi.org/10.1016/j.phrs.2009.01.017.
[33] S. Nakashima, Y. Hiraku, S. Tada-Oikawa, T. Hishita, E.C. Gabazza, S. Tamaki, S. Kawanishi, Vacuolar H^+-ATPase inhibitor induces apoptosis via lysosomal dysfunction in the human gastric cancer cell line MKN-1, J. Biochem. 134 (2003) 359–364, https://doi.org/10.1093/jb/mvg153.
[34] T. Kawaguchi, K. Miyazawa, S. Moriya, T. Ohtomo, X.F. Che, M. Naito, M. Itoh, A. Tomoda, Combined treatment with bortezomib plus bafilomycin A1 enhances the cytocidal effect and induces endoplasmic reticulum stress in U266 myeloma cells: crosstalk among proteasome, autophagy-lysosome and ER stress, Int. J. Oncol. 38 (2011) 643–654, https://doi.org/10.3892/ijo.2010.882.
[35] V. Michel, Y. Licon-Munoz, M. Trujillo Bisoffi, K.J. Parra, Inhibitors of vacuolar ATPase proton pumps inhibit human prostate cancer cell invasion and prostate specific antigen expression and secretion, Int. J. Cancer 132 (2013) E1–10, https://doi.org/10.1002/ijc.27811.
[36] F. Kobia, S. Duchi, G. Deflorian, T. Vaccari, Pharmacologic inhibition of vacuolar H^+ ATPase reduces physiologic and oncogenic notch signaling, Mol. Oncol. 8 (2014) 207–220, https://doi.org/10.1016/j.molonc.2013.11.002.
[37] M. Pérez-Sayans, J.M. Somoza-Martin, F. Barros-Angueira, J.M. Rey, A. García-García, V-ATPase inhibitors and implication in cancer treatment, Cancer Treat. Rev. 35 (2009) 707–713, https://doi.org/10.1016/j.ctrv.2009.08.003.
[38] T. Azzarito, G. Venturi, A. Cesolini, S. Fais, Lansoprazole induces sensitivity to suboptimal doses of paclitaxel in human melanoma, Cancer Lett. 356 ((2015) 697–703, https://doi.org/10.1016/j.canlet.2014.10.017.
[39] S. Taylor, E.P. Spugnini, Y.G. Assaraf, T. Azzarito, T., C. Rauch, and Fais, S. Microenvironment acidity as a major determinant of tumor chemoresistance: Proton pump inhibitors (PPIs) as a novel therapeutic approach. Drug Resist. Updat. 23 (2015) 69–78. Doi: https://doi.org/10.1016/j.drup.2015.08.0041
[40] D. Grossman, D.C. Altieri, Drug resistance in melanoma: Mechanisms, apoptosis, and new potential therapeutic target, Cancer Metastasis Rev. 20 (2001) 3–11, https://doi.org/10.1023/A:1013123532723.
[41] X.D. Zhang, J.J. Wu, S. Gillespie, J. Borrow, P. Hersey, Human melanoma cells selected for resistance to apoptosis by prolonged exposure to tumor necrosis factor-related apoptosis-inducing ligand are more vulnerable to necrotic cell death induced by cisplatin, Clin. Cancer Res. 12 (2006) 1355–1364, https://doi.org/10.1158/1078-0432.CCR-05-2084.
[42] S. Fan, Y. Niu, N. Tan, Z. Wu, Y. Wang, H. You, R. Ke, J. Song, Q. Shen, W. Wang, G. Yao, H. Shu, H. Lin, M. Yao, Z. Zhang, J. Gu, W. Qin, LASS2 enhances chemosensitivity of breast cancer by counteracting acidic tumor microenvironment through inhibiting activity of V-ATPase proton pump, Oncogene 32 (2013) 1682–1690, https://doi.org/10.1038/onc.2012.183.
[43] S. Fais, Evidence-based support for the use of proton pump inhibitors in cancer therapy, J. Transl. Med. 13 (2015) 368, https://doi.org/10.1186/s12967-015-0735-2.
[44] W. Shen, X. Zou, M. Chen, P. Lui, Y. Shen, S. Huang, H. Guo, L. Zhang, Effects of diphyllin as a novel V-ATPase inhibitor on gastric adenocarcinoma, Eur. J. Pharmacol. 667 (2011) 330–338, https://doi.org/10.1016/j.ejphar.2011.05.042.
[45] P. Williamson, R.A. Schlegel, Transbilayer phospholipid movement and the clearance of apoptotic cells, Biochim. Biophys. Acta 1585 (2002) 53–63, https://doi.org/10.1016/S1388-1981(02)00324-4.
[46] D.V. Krysko, T. Vanden Berghe, E. Parthoens, K. D'Herde, P. Vandenabeele, Methods for distinguishing apoptotic from necrotic cells and measuring their clearance, Methods Enzymol. 442 (2008) 307–341, https://doi.org/10.1016/S0076-6879(08)01416-X.
[47] R. Supino, G. Petrangolini, G. Pratesi, M. Tortoreto, E. Favini, D.L. Bo, P. Casalini, E. Radaelli, A.C. Croce, G. Bottiroli, P. Misiano, C. Farina, F. Zunino, Antimetastatic effect of a small-molecule vacuolar H^+- ATPase inhibitor in *in vitro* and *in vivo* preclinical studies, J Pharmacol Exp Therap. 324 (2008) 15–22, https://doi.org/10.1124/jpet.107.128587.
[48] A.V. Turina, M.V. Nolan, J.A. Zygadlo, M.A. Perillo, Natural terpenes: self-assembly and membrane partitioning, Biophys. Chem. 122 (2006) 101–113, https://doi.org/10.1016/j.bpc.2006.02.007.
[49] B. Singh, R.A. Sharma, Plant terpenes: defense responses, phylogenetic analysis, regulation and clinical applications, 3 Biotech. 5 (2015) 129–151, https://doi.org/10.1007/s13205-014-0220-2.